Comparing Multiple Exciton Generation in Quantum Dots To Impact Ionization in Bulk Semiconductors: Implications for Enhancement of Solar Energy Conversion

ARTICLE *in* NANO LETTERS · AUGUST 2010

Impact Factor: 13.59 · DOI: 10.1021/nl101490z · Source: PubMed

NANO LETTERS

pubs.acs.org/NanoLett

Comparing Multiple Exciton Generation in Quantum Dots To Impact Ionization in Bulk Semiconductors: Implications for Enhancement of Solar Energy Conversion

Matthew C. Beard,*,† Aaron G. Midgett,†,‡ Mark C. Hanna,† Joseph M. Luther,† Barbara K. Hughes,†,‡ and Arthur J. Nozik†,‡

†Basic Sciences Center, National Renewable Energy Laboratory, Golden, Colorado 80401 and ‡Department of Chemistry and Biochemistry, University of Colorado, Boulder, Boulder, Colorado 80309

ABSTRACT Multiple exciton generation (MEG) in quantum dots (QDs) and impact ionization (II) in bulk semiconductors are processes that describe producing more than one electron−hole pair per absorbed photon. We derive expressions for the proper way to compare MEG in QDs with II in bulk semiconductors and argue that there are important differences in the photophysics between bulk semiconductors and QDs. Our analysis demonstrates that the fundamental unit of energy required to produce each electron−hole pair in a given QD is the band gap energy. We find that the efficiency of the multiplication process increases by at least 2 in PbSe QDs compared to bulk PbSe, while the competition between cooling and multiplication favors multiplication by a factor of 3 in QDs. We also demonstrate that power conversion efficiencies in QD solar cells exhibiting MEG can greatly exceed conversion efficiencies of their bulk counterparts, especially if the MEG threshold energy can be reduced toward twice the QD band gap energy, which requires a further increase in the MEG efficiency. Finally, we discuss the research challenges associated with achieving the maximum benefit of MEG in solar energy conversion since we show the threshold and efficiency are mathematically related.

KEYWORDS Multiple exciton generation, carrier multiplication, solar energy conversion, semiconductor nanocrystals, quantum dots

Electron−hole pair multiplication (EHPM) occurs when more than one electron−hole pair (EHP) is produced by absorption of one photon with energy at least twice the semiconductor band gap, E_g. In bulk semiconductors, EHPM is referred to as impact ionization (II), a well-known phenomenon,[1,2] while in semiconductor nanocrystals, or quantum dots (QDs), EHPM is referred to as multiple exciton generation, MEG,[3] carrier multiplication, CM,[4] or direct carrier multiplication, DCM,[5] to distinguish the phenomenon from II and highlight new proposed physics in quantum confined systems. In recent years, MEG has been reported in several QDs, such as PbSe,[3,4,6−8] PbS,[3,9] PbTe,[10] Si,[11] CdSe,[12−14] InAs,[15,16] InP,[17] and CdTe/CdSe core−shell QDs.[18] However, some authors report they cannot reproduce MEG in CdSe[19] and InAs[20,21] QDs, and for the lead chalcogenides, where MEG has been reported by all investigators, there is controversy concerning the value of the quantum yields (QYs) as well the significance of MEG for improving the performance of photovoltaic cells. Some authors report QYs ≫ 1 for exciton formation in PbSe and PbS QDs,[3,4,6,7,22,23] while others have reported only small QYs (<1.25).[8] These variations have been attributed to effects of surface chemistry on the exciton relaxation dynamics[8,23] and in some cases to long-lived charging of the QDs caused by trapping of a photoexcited electron or hole at the QD surface leaving a delocalized hole or electron residing in the core.[22] Extraneous effects such as charging can be reduced by flowing,[24] or stirring the sample[22] during the experiment and using low photon fluencies.

An enhancement in EHPM is expected in QDs over that achievable in bulk semiconductors due to beneficial quantum size effects, such as, relaxed momentum conservation, modified carrier-cooling rates, and enhanced Auger processes. In a recent report,[25] EHPM in bulk films of PbSe and PbS was measured using time-resolved terahertz spectroscopy, and the QYs, or number of electron−hole pairs produced per absorbed photon, were compared with previous reports of MEG in QDs of PbSe and PbS. The authors found that plots of the QYs of EHPM for the bulk semiconductors were equivalent or even larger than that reported for QDs for a given photon energy. From that comparison, the authors concluded that EHPM processes are not enhanced in QDs and EHPM processes are unlikely to significantly enhance solar energy conversion by boosting the photocurrent. In this report, we discuss what we claim is the appropriate way to compare MEG in QDs with II in bulk semiconductors. We show that plotting QY vs $h\nu/E_g$ (where E_g is the band gap) provides information about the competition between producing multiple carriers and other energy

* To whom correspondence should be addressed, matt.beard@nrel.gov.
Received for review: 04/27/2010
Published on Web: 07/26/2010

DOI: 10.1021/nl101490z | *Nano Lett.* **2010,** *10,* 3019–3027

relaxation channels. We present a rigorous derivation of the efficiency of EHPM, η_{EHPM}, whether for bulk semiconductors or QD samples, that allows for meaningful comparisons and shows how η_{EHPM} is related to both the threshold energy needed to produce extra EHPs, $h\nu_{th}$, and the competition between EHPM and other relaxation channels. We find η_{EHPM} increases by ~2 in PbSe QDs compared to bulk PbSe. We discuss differences in the photophysics between MEG and II. Finally, we present thermodynamic detailed balance calculations, following the Shockley–Queisser analysis,[26−28] that demonstrate power conversion efficiencies in QD solar cells can greatly exceed that of their bulk semiconductor counterparts.

The recent report[25] on EHPM in bulk PbS and PbSe and a previous report on MEG in PbS and PbSe QDs[8] compare EPHM for bulk semiconductors and QDs on plots of QY vs absolute photon energy ($h\nu$). Such a comparison is misleading and incorrect, because for proper comparisons it is necessary to determine η_{EHPM}. The efficiency, η_{EHPM}, is defined as the minimum amount of energy required to produce an EHP (i.e., the band gap), divided by the actual amount of energy required to produce an additional EHP after the MEG threshold is passed; the latter quantity is referred to in the literature as the electron–hole pair creation energy ε_{EHPM};[29,30] $\eta_{EHPM} = E_g/\varepsilon_{EHPM}$. The fact that measurements of MEG QYs for PbSe and PbS QDs are at best equal to that found in the recent II measurements[20] when compared using $h\nu$ scaling, does not imply an absence of quantum confinement effects or that EHPM is the same for QDs and bulk. Furthermore, QY data plotted vs $h\nu$ does not provide information about η_{EHPM}. When $h\nu$ scaling is used, only the electron–hole pair creation energy, ε_{EHPM}, can be ascertained from such a plot; ε_{EHPM} is equal to the inverse of the slope of QY vs $h\nu$, $[\varepsilon_{EHPM} = (\Delta QY/\Delta h\nu)^{-1}]$. In contrast, as we will show below, the slope of QY vs $h\nu/E_g$, is equal to the EHPM efficiency, $\eta_{EHPM} = [\Delta QY/\Delta(h\nu/E_g)]$. Thus, η_{EHPM} is a measure of how well EHPM competes with other relaxation channels and provides a proper and meaningful comparison with respect to the photophysics of EHPM.

EHPM Energy Considerations and Efficiency. A fundamental constraint for EHPM processes is the conservation of energy, and for systems with translational symmetry (bulk crystals) the conservation of momentum must also be satisfied. An energetic electon–hole pair, EHP*, produced by absorption of a photon with sufficient excess energy above the band gap can produce m EHPs. The EHPM process is described by the scheme

$$EHP^* \xrightarrow{EHPM} me + mh \qquad (1)$$

When an EHP* is produced by absorption of a photon with energy, $h\nu > E_g$, conservation of energy dictates that the total number of EHPs created, multiplied by their energy, must be less than or equal to the total input energy (energy of absorbed photons)

$$N(EHP)\varepsilon(e{\bullet}h) \le h\nu N_{photons} \qquad (2)$$

where $\varepsilon(e \cdot h)$ is defined as the thermalized energy of an EHP (i.e., the band gap). The inequality reflects the fact that some input energy is lost to heat. For photon energies greater than E_g and in the absence of EHPM, all the excess energy is lost as heat. The energy loss per absorbed photon is $E_{loss} = \Delta E_{tot} = (h\nu - E_g)$. For EHPM, the excess energy must be greater than the electron–hole pair creation energy, $\Delta E_{tot} \ge \varepsilon_{EHPM}$. In the ideal case the efficiency equals 1, $\eta_{EHPM} = 1$, and the amount of energy needed to produce an additional EHP is the band gap energy, $\varepsilon_{EHPM} = E_g$. Therefore, when the photon energy reaches $2E_g$ one additional EHP can be created utilizing all excess energy, thus, $E_{loss} = 0$ at $h\nu = 2E_g$. For photon energies exceeding $2E_g$, but less than $3E_g$, one additional EHP is formed and the rest is lost to heat, and $E_{loss} = h\nu - 2E_g$,which is the total lost energy after one EHPM event. At $h\nu = 3E_g$, two additional EHPs can be produced with $E_{loss} = 0$. Generalizing these observations, the total energy lost is $E_{loss}^{(m)} = h\nu - mE_g$,where m is the total number of EHPs allowed by energy conservation with a photon energy of $h\nu$, thus $m = \lfloor h\nu/E_g \rfloor$, where the operator, $\lfloor\rfloor$, denotes rounding down to the nearest integer.[31] In general, the amount of energy loss, E_{loss} is the total excess energy minus the number of EHPs multiplied by the energy needed to produce additional EHPs

$$E_{loss} = (h\nu - E_g) - (m - 1)E_g = (h\nu - mE_g) \qquad (3)$$

for

$$mE_g \le h\nu < (m + 1)E_g$$

where eq 3 is the energy loss for absorption of one photon. Solving for the quantum yield, we find $QY = m = [h\nu/E_g]$ and resembles a staircase that is shown as trace M_{max}, in Figure 1b.

For nonideal cases, more energy than the band gap is needed to produce an additional EHP, $\varepsilon_{EHPM} > E_g$, and this nonideality is reflected in EHPM efficiencies less than 1, $\eta_{EHPM} < 1$. Therefore, $m = 1$ for photon energies less than $E_g + \varepsilon_{EHPM}$ and, $m = 2$ for photon energies greater than $E_g + \varepsilon_{EHPM}$ but less than $E_g + 2\varepsilon_{EHPM}$. This can be generalized as above to find the maximum number of EHPs at a given photon energy.

$$\begin{aligned} E_{loss} &= (h\nu - E_g) - (m - 1)\varepsilon_{EHPM} \\ &= h\nu - (E_g + (m - 1)\varepsilon_{EHPM}) \end{aligned} \qquad (4)$$

DOI: 10.1021/nl101490z | Nano Lett. 2010, 10, 3019–3027

for

$$E_g + (m+1)\varepsilon_{EHPM} \le h\nu \le E_g + m\varepsilon_{EHPM}$$

where m is the total allowed EHPs for the nonideal case. Substituting $\varepsilon_{EHPM} = E_g/\eta_{EHPM}$ and solving eq 4 when $E_{loss} = 0$, we find $m = \lfloor (h\nu/E_g - 1)\eta_{EHPM} \rfloor + 1$, and therefore the maximum QY is,

$$QY_{max} = \left\lfloor \left(\frac{h\nu}{E_g} - 1 \right) \eta_{EHPM} \right\rfloor + 1 \qquad (5)$$

Typically, experimental QYs for EHPM start at some energy threshold, $h\nu_{th}$, and increase linearly, rather than exhibiting the staircase features described above that leads to eq 5. In these soft threshold cases, a phenomenological extension of eq 5 can be made by assuming that the energy loss is equal to $E_{loss} = h\nu_{th} - E_g$ for photon energies greater than $E_g + \varepsilon_{EHPM}$. Substituting $E_{loss} = (h\nu_{th} - E_g)$into eq 4 and solving for m we find

$$QY = \left(\frac{h\nu}{E_g} - 1 \right) \eta_{EHPM} \qquad (6)$$

By solving eq 5 or 6 for when the QY ≥ 1, we find that the energy threshold,$h\nu_{th}$, is related to η_{EHPM}, and is

$$h\nu_{th} = E_g + E_g/\eta_{EHPM} \qquad (7)$$

The total energy loss is $E_{loss} = h\nu_{th} - E_g = E_g/\eta_{EHPM}$. From the arguments above we conclude that η_{EHPM} is obtained from slope of QY vs $h\nu/E_g$.

EHPM Rates vs Cooling Rate. We also consider the competition between the rate of EHPM, k_{EHPM}, vs alternative energy relaxation channels, such as cooling via phonon emission. Figure 1a shows a cascading kinetic scheme where the high-energy exciton either cools directly to the lowest state or produces a hot biexciton state, n_2*. That state can either cool or undergo another EHPM event. The initially excited exciton eventually loses all of its excess energy. We do not include decay processes of the relaxed excitons such as Auger recombination and radiative recombination that we assume occur on longer time scales. The set of differential equations that describe the cascaded scheme shown in Figure 1 are

$$\begin{aligned}
\dot{n}_1^* &= k_{cool} n_1^* - k_{EHPM} n_1^* + I_o \\
\dot{n}_1 &= k_{cool} n_1^* \\
\dot{n}_2^* &= k_{EHPM}^{(1)} n_1^* - k_{cool} n_2^* - k_{EHPM}^{(2)} n_2^* \\
\dot{n}_2 &= k_{cool} n_2^* \\
\dot{n}_3^* &= k_{EHPM}^{(2)} n_2^* - k_{cool} n_3^* - k_{EHPM}^{(3)} n_3^* \qquad (8) \\
&\vdots \\
\dot{n}_m^* &= k_{EHPM}^{(m-1)} n_{m-1}^* - k_{cool} n_m^* - k_{EHPM}^{(m)} n_m^* \\
\dot{n}_m &= k_{cool} n_m^*
\end{aligned}$$

where I_o is the photon fluence, n_1^* is the population of hot single exciton states, n_1 is the population of relaxed single exciton states, n_2^* is the population of hot biexciton states n_2 is the population of relaxed biexciton states, n_3^* is the population of hot triexciton states, and n_3 is the population of relaxed triexciton states. In general, n_m^* is the hot m-exciton state and n_m is the cooled m-exciton state. The cooling rate is denoted k_{cool}, and the EHPM rates are denoted $k_{EHPM}^{(r)}$, where $r = m - 1$. To find the QY, we solve eq 8 for the population of single, bi-, tri-, and higher exciton states at times longer than EHPM and cooling

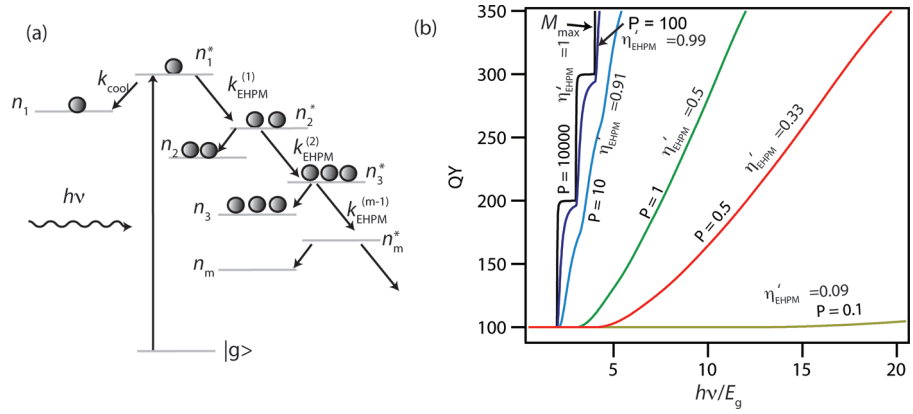

FIGURE 1. (a) Cascade scheme for EHPM considered here. A high-energy photon creates an exciton with excess energy, n_1*. The hot exciton can lose energy by cooling or EHPM to form either n_1 or a hot biexciton, n_2* and so on. (b) Plots of eq 9 for different values of P, η'_{EHPM} is shown at each P value.

DOI: 10.1021/nl101490z | Nano Lett. 2010, 10, 3019–3027

$$QY = \sum_{j=1}^{m} j n_j(t > \tau_{EHPM}, \tau_{cool}) = \sum_{j=1}^{m} j \frac{k_{cool} \prod_{i=1}^{j} k_{EHPM}^{(i-1)}}{\prod_{i=1}^{j} (k_{cool} + k_{EHPM}^{(i)})} \quad (9)$$

where $k_{EHPM}^{(0)} = 1$. To use eq 9 we need to know how k_{EHPM} and k_{cool} vary with excess energy. Keldysh found that for bulk semiconductors the EHPM rate follows[32,33]

$$k_{EHPM} = \left(\frac{e^2}{4\pi\varepsilon}\right)\frac{m_e^*}{h^3}\frac{I_c^2 I_v^2}{(1+2\gamma)^{3/2}}\frac{(h\nu - h\nu_{th})^2}{h\nu_{th}^2} \quad (10)$$

where I_c and I_v are the overlap integrals between initial and final states in the conduction and valence bands and $\gamma = m_e^*/m_h^*$ which are the effective masses in the conduction and valence bands. Now we need to know how k_{cool} varies with excess energy.

For bulk semiconductors, the most important cooling relaxation channel is hot carrier cooling via phonon emission, k_{phonon}. The ratio of rates, k_{EHPM}/k_{phonon} is proportional to the ratio of the mean free path for phonon scattering, λ_{phonon} and the mean free path for EHPM, λ_{EHPM}, i.e., $\lambda_{EHPM}/k_{phonon} \propto \lambda_{phonon}/\lambda_{EHPM}$. We can get an idea of the length scales by considering the behavior of free charge carriers in bulk semiconductors. The average distance a charge carrier travels prior to phonon scattering is equal to the velocity of the carrier multiplied by the average time between collisions, $\lambda_{phonon} = v\langle\tau\rangle$. λ_{phonon} is relatively independent of the kinetic energy of the charged carrier because the length scale for phonon scattering is determined by the properties of the lattice, so as v increases it is offset by a shorter $\langle\tau\rangle$. For bulk PbSe, λ_{phonon} can be estimated from the carrier mobility, and we find $\lambda_{phonon} \sim 67$ nm. In bulk semiconductors, λ_{EHPM} decreases with increasing carrier velocity (or excess kinetic energy),[34] corresponding to an increasing k_{EHPM}. In bulk PbSe, λ_{EHPM} has not been measured to our knowledge; however, for Si $\lambda_{EHPM} \sim 10$ nm[30] at a few electronvolts above the band edge and for GaAs, $\lambda_{EHPM} > 10$ nm for excess energies between 1 and 10 eV.[34] In accordance with the above observations, a Monte Carlo simulation of phonon cooling and impact ionization finds the phonon relaxation rate to be independent of excess energy, while the II rate increased with increasing excess energy.[35] The dimensions of QDs studied here are smaller than both λ_{phonon} and λ_{EHPM} of bulk materials indicating that EHPM and cooling in QDs are most likely different from bulk. Following Ridley[32] we parametrize k_{EHPM}/k_{cool} by the following expression

$$k_{EHPM} = k_{cool} P \left(\frac{h\nu - h\nu_{th}}{h\nu_{th}}\right)^s \quad (11)$$

where the factor P determines whether the EHPM onset is hard or soft, for $P \gg 1$ the onset is hard, and for $P < 1$ the onset is soft. The exponent s in eq 11 was found to be 2 in the original Keldysh treatment. However, that treatment was for an ideal semiconductor; in more detailed treatments, s can vary between 2 and 5. In our treatment we allow both s and P to be adjustable parameters. We now define an efficiency, η'_{EHPM}, based on the threshold parameter, P, that captures the competition between the k_{EHPM} and k_{cool}

$$\eta'_{EHPM} = \frac{P}{1+P} \quad (12)$$

where we use the prime to distinguish η'_{EHPM} from η_{EHPM} defined above in terms of ε_{EHPM}. The relationship between η'_{EHPM} and the energy threshold is the same as we found before, but now each EHPM event has its own energy threshold given by

$$h\nu_{th}^{(m)} = E_g(1 + m/\eta'_{EHPM}) \quad (13)$$

where $k_{EHPM}^{(m)}$ is zero below $h\nu_{th}$ and therefore $k_{EHPM}^{(m)} = k_{cool}P[(h\nu - h\nu_{th}^{(m)})/h\nu_{th}]^s\theta(h\nu - h\nu_{th}^{(m)})$ where θ is the heavyside step function.

In Figure 1b we show plots of the QY from eq 9 for various values of P (with $s = 2$) and note the values of η'_{EHPM}. We vary P from 10000 to 0.1, at $P = 10000$, $\eta'_{EHPM} = 1$, and EHPM dominates over cooling. For this scenario, we recover the staircase behavior for an ideal behavior where eq 3 gives the total energy loss. At $P = 1$, $\eta'_{EHPM} = 0.5$, we find a roughly linear increase of the QY with $h\nu/E_g$; the onset, however, is not as sharp as that predicted from eq 6. For QY values less than ~150 % and for $P < 10$, $k_{cool} > k_{EHPM}$, and QY increases ~ quadratically with $h\nu/E_g$. At a QY = 150 %, $k_{cool} \approx k_{EHPM}$, this can been seen by substituting $k_{cool} = k_{EHPM}$ and considering the first two terms of eq 9, $QY = k_{cool}/(k_{cool} + k_{EHPM}^{(1)}) + 2k_{EHPM}^{(1)}/(k_{cool} + k_{EHPM}^{(1)})$. The QY in this energy range increases approximately linear with $h\nu/E_g$ with a slope determined by P and s.

Data Analysis. Figure 2a displays recent MEG QY data reported in ref 24 for three samples of different sizes of PbSe QDs (filled brown squares). We employ a 1 mm flow cell and flow our samples at 150 mL/min during the transient absorption experiment. We also plot recent data reported in ref 22 where the samples were stirred rather than flowed. The good agreement between these two data sets provides confidence in our reported results. EHPM QYs for bulk PbSe (filled black squares) and bulk PbS (open circles) are plotted

DOI: 10.1021/nl101490z | Nano Lett. 2010, 10, 3019--3027

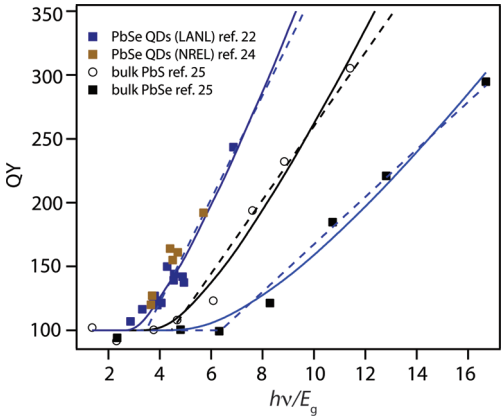

FIGURE 2. QY vs $h\nu/E_g$ for PbSe QD samples measured at LANL and reported in ref 22 (blue squares), and PbSe QDs measured at NREL and reported in ref 24 (brown squares). EHPM QYs for bulk PbSe and bulk PbS are reproduced from ref 25. The dotted lines are a linear-least-squares best fit of eq 6 to the data, and the solid lines are eq 9. The best-fit parameters are reported in Table 1.

TABLE 1. Best-Fit Parameters for Lines Shown in Figure 2

	η_{EHPM}	$h\nu_{th}$	η'_{EHPM}	P	s	$h\nu'_{th}$
bulk PbSe	0.19	6.5 E_g	0.31	0.45	2.5	4.22 E_g
bulk PbS	0.29	4.4E_g	0.45	0.83	2.6	3.22 E_g
QD samples						
PbSe QDs	0.41	3.4E_g	0.6	1.5	2.2	2.7E_g

and reproduced from ref 25. These data points were measured using a time-resolved terahertz experiment that is sensitive to the total number of carriers produced by the excitation pulse. Equation 6 was fit to each data set with only one adjustable parameter, η_{EHPM}, to obtain both the slope and $h\nu_{th}$ and are shown as dotted lines. The solid lines are the best-fit lines using eq 9 where P and s are allowed to vary. The fits using eq 9 are slightly better because the predicted onset is not as abrupt. This appears to be more important for the QD samples than the bulk data. We report the best-fit parameters in Table 1 and tabulate η'_{EHPM},$h\nu_{th}$, and $h\nu'_{th}$.

The efficiency, η_{EHPM}, is clearly better for the PbSe QD samples than for the bulk PbSe. We find η_{EHPM} increases from 0.19 to 0.41 in the QD samples (a factor of >2), while P increases from 0.45 to 1.5, an increase of >3. In accordance with our discussion above, $h\nu_{th}$ decreases from 4.2E_g to 2.7E_g. Through the analysis presented here, comparing EHPM as a function of $h\nu/E_g$ is more meaningful and correct than using $h\nu$. One of the reasons why there is confusion concerning $h\nu$ vs $h\nu/E_g$ scaling is because a proper definition of η_{EHPM} had not been clearly established. The assumption that the MEG efficiency is equal to the enhanced QY at a particular photon excitation energy leads to an erroneous conclusion that because the QY decreases at some fixed excitation energy for smaller QDs that η_{EHPM} is lower for QDs compared to bulk semiconductors. This leads an incorrect conclusion that EHPM is lower in QD than in bulk semiconductors. However, this definition of the efficiency neglects the energetics involved. The excess energy available to produce an additional EHP decreases for smaller QD sizes because band gap energy increases for QDs compared to bulk. Therefore, $h\nu/E_g$ scaling provides a clear way of comparing EHPM while the $h\nu$ scaling does not. Furthermore, when considering data using the $h\nu$ scaling, the relationship between the threshold values and η_{EHPM} is obscured because there does not appear to be any correlation between the slope (or the inverse of the electron−hole pair creation energy) and $h\nu_{th}$. However, the correlation is clearly visible with the $h\nu/E_g$ scaling. For example, considering the bulk PbS data we see it takes ~4.3E_g for EHPM to begin and each new EHP occurs at each additional 3.3E_g, in accordance with $\eta_{EHPM} = 0.29$. The recent report from Delerue et al.[36] also concluded that η_{EHPM} (defined in a similar fashion as we define here) is enhanced in QDs relative to bulk semiconductors.

EHPM Energy Threshold Considerations. In the above analysis, we find a relationship between η_{EHPM} and $h\nu_{th}/E_g$. This relationship implies that $h\nu_{th}$ is inextricably linked to η_{EHPM}. However, the link between the $\eta_{EHPM}$and $h\nu_{th}$ can be broken if other factors besides the efficiency help determine $h\nu_{th}$. For example, if the relationship between ε_{EHPM} and the band gap energy is $\varepsilon_{EHPM} = AE_g + B$ where B is the related to $h\nu_{th}$.[29,30,37] We could also consider a scenario where ε_{EHPM} is not a linear function but varies with the amount of excess energy so that η_{EHPM} increases with increasing energy, again plotting QY vs $h\nu_{th}/E_g$ will provide η_{EHPM}.

There are at least three possible contributions to $h\nu_{th}$: (1) conservation of energy, (2) conservation of momentum, and (3) η_{EHPM}, as discussed above. Energy conservation dictates that $h\nu_{th}/E_g \geq 2$; however, in a bulk semiconductor, $\Delta k = 0$ absorption selection rules increases $h\nu_{th}$. The excess energy in the conduction band is $\Delta E_e = (h\nu - E_g)\ (1 + m_e/m_h)$ and $\Delta E_h = (h\nu - E_g) - \Delta E_e$, where m_e is the effective mass of the electron and m_h is the effective mass of the hole. For parabolic bands, $m_e \approx m_h$, the situation for PbS and PbSe, and $h\nu_{th}/E_g \approx 3$ on energy conservation arguments alone. However, the bands may not be parabolic; $h\nu_{th}$ depends upon the detailed band structure and there is a distribution of excess energies populated by absorption.[38] There may also be weak second-order transitions involving a phonon that relaxes the $\Delta k = 0$ selection rule.

Crystal momentum must be conserved for systems with translational symmetry and this additional constraint increases $h\nu_{th}$ over the energy conservation limit for bulk semiconductors. The amount of increase in $h\nu_{th}$ depends on the band structure, positions of split-off bands, indirect vs direct transitions, and other details that pertain to the semiconductor of interest. A review of the most common situations found in semiconductors has been tabulated in ref 2. For the case of isotropic bands the excess energy in the conduction or valence band is given by

DOI: 10.1021/nl101490z | *Nano Lett.* **2010,** *10,* 3019–3027

$$\Delta E_e = \frac{(2m_e + m_h)}{m_e + m_h} E_g \quad (14)$$

where ΔE_e is the excess kinetic energy necessary in the initiating electron. For PbS and PbSe the above condition results in an excess energy of $3E_g/2$, $E_g/2$ above the energy conservation limit. Therefore, energy and momentum constrain $h\nu_{th}/E_g \approx 4$ for PbSe and PbS. In QDs, momentum is no longer a good quantum number since a crystal lattice only exists for a few nanometers and therefore the momentum conservation limit is relaxed, and for PbSe QDs, $h\nu_{th}$ has been observed to be $3\tilde{E}_g$ (reported here as $2.7E_g$), well below the momentum conservation limit. Thus one major advantage of QDs is the possibility to decrease $h\nu_{th}$ below the momentum conservation limit defined for bulk systems.

Photophysics of Hot Electrons and Quantum Confinement Effects. The analysis of η_{EHPM} presented above demonstrates that EHMP is more efficient in PbSe QDs than in bulk PbSe. In QDs there are at least three fundamental properties that are modified due to quantum confinement and affect the EHPM process.

(A) Crystal momentum is no longer a good quantum number. There are three factors that can affect $h\nu_{th}$ related to crystal momentum: (1) absorption selection rules are modified; (2) conservation of crystal translational momentum is relaxed, allowing $h\nu_{th}$ to be less than that required by momentum conservation. In fact, we find $h\nu_{th}$ in QDs of PbSe is lower than that allowed by momentum conservation in bulk PbSe, and (3) single and mutliexcitonic states can be coupled through the Coloumb operator to form a superposition of states.[39] Such coupling is not possible in bulk systems with well-defined momentum.

(B) The discrete structure of semiconductor QD energy bands, due to quantum confinement and intimate control over surface states and surface ligands can be used to modify carrier relaxation rates and thereby increase P. Intimate control over variable surfaces and interactions is a research challenge and opportunity rather than a priori a bad characteristic.

(C) Increased Coulombic coupling between excitons in QDs increases Auger-related processes like MEG.

The theoretical model for MEG developed by Efros, Shabaev, and Nozik[39] shows how the photophysics governing MEG in QDs is new and different from EHPM in bulk semiconductors. The strong Coulomb coupling of multiple excitons driving MEG in QDs is not present in the bulk. Other models for MEG/CM[49,50] also show different physics for bulk semiconductors compared to QDs. For example, in the Klimov model, CM occurs through excitation of virtual states that are transferred to biexciton states via intraband transitions. η_{EHPM} is higher in QDs because of enhanced intraband transition oscillator strengths in QDs vs bulk semiconductors. Zunger et al. use an impact ionization approach to calculate enhancements in EHPM in QDs due to a higher density of final states.[51]

Our analysis of η_{EHPM} presented here does not consider whether k_{EHPM} is enhanced in QDs over bulk or whether k_{cool} decreases, and quantum confinement may effect both k_{cool} and k_{EHPM}. As we noted earlier the length scales for both EHPM and cooling in bulk PbSe are larger than the QD diameter; therefore we expect some dependence of these processes with size. If no new physical processes are invoked, then we would expect the surfaces of the QDs to dominate these relaxation pathways. The photoexcited carrier should reach the QD surface balistically, and both k_{cool} and k_{EHPM} could increase. The resulting QY would depend on whether k_{EHPM}/k_{cool} increased, decreased, or remained constant. However, size effects do introduce new relaxation pathways that are not found in corresponding bulk semiconductors. One of the arguments for enhanced EHPM in QDs is the sparse density of states that can slow or inhibit phonon-mediated relaxation (referred as the phonon bottleneck).[40,41] The presence of the phonon bottleneck is masked by enhanced Coulombic coupling between the electron and hole wave functions providing an Auger-like relaxation channel[42] that relies on a large difference in m_e and m_h. Slowed cooling has been observed in QD systems where the electron and hole are separated,[43] the effective masses are similar,[44] or surface relaxation channels are suppressed;[45] combining these approaches, the 1P to 1S cooling was slowed to ~1 ns.[46] However, the majority of hot carrier relaxation studies have used low excess energies, while MEG measurements are performed at high excess energies. One of the criticisms of enhanced MEG in QDs is that the density of states at these high excess energies is sufficiently dense to allow fast relaxation via phonon emission (the absorption spectra of QDs approach that of bulk at high excess energies[47]). However, we argue that it is the relative length scales that are important, and as we have shown, the ratio increases for QDs. It stands to reason that QD surfaces play a significant role in all carrier relaxation processes at these high energies. Recent theoretical treatments of QD−ligand interactions demonstrate that the QDs cannot be considered as isolated semiconductors within very high barrier confinement levels.[48] A significant research challenge is to better understand these high excess energy states and to determine what factors may influence MEG vs other relaxation channels and thereby learn how to further increase P. The majority of theoretical treatments of MEG to date have only considered enhancements in k_{EHPM} and not the ratio of k_{EHPM}/k_{cool}.

Implications for Improved Solar Energy Conversion. Concerning the issue of whether MEG can enhance solar power conversion efficiencies, we now demonstrate that solar cells produced from QDs can have much higher power conversion efficiencies than their bulk counterparts. The results are based on Shockley−Queisser (SQ) detailed balance calculations and are summarized in Figure 3. We[28] and

DOI: 10.1021/nl101490z | Nano Lett. 2010, 10, 3019--3027

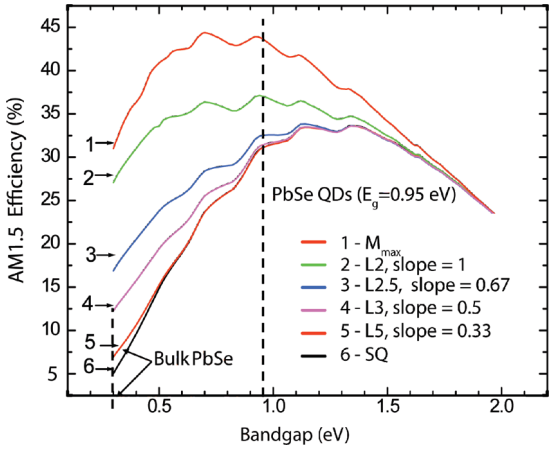

FIGURE 3. Photovoltaic power conversion efficiencies at AM1.5 vs band gap for various characteristics of MEG QY. Curve SQ is the Shockley−Queisser limit, and curves L2, L2.5, L3, L5, and M_{max} are defined in the text.

Klimov[52] have previously conducted thermodynamic efficiency calculations comparing bulk semiconductors and QDs using the approach, and we extend theses calculations for various values of $h\nu_{th}$ and η_{EHPM}. In Figure 3, curve 6 (black solid line) is the conventional SQ calculation with just 1 EHP created per photon at the band gap; curve 1 (solid red curve) assumes the maximum multiplication energetically allowed and is based on M_{max}. Curve 2 (solid green line) is based on $h\nu_{th} = 2E_g$ followed by creation of one extra exciton created per E_g (defined as the L2 characteristic); curve 3 (solid blue line) is based on a threshold of $2.5E_g$ with slope defined in eq 6, curve 4 is based on a threshold of $3E_g$ (defined as the L3 characteristic); curve 5 is based on a threshold of $4.5E_g$ with $\eta_{EHPM} = 0.19$ (defined as the L5 characteristic and is the experimental bulk characteristic for PbSe, see Figure 2b). For each LX case E_g/η_{EHPM} is lost to heat as discussed above (eq 6). Our analysis suggests that the slope has a smaller effect on power conversion efficiency than does $h\nu_{th}$. Thus identifying QD systems where $h\nu_{th}$ can be lowered (also implying a higher η_{EHPM}) is imperative.

As seen in Figure 3, the maximum thermodynamic conversion efficiency of ~5% for bulk PbSe is only marginally enhanced when the experimentally measured EHPM is included. Thus, EHPM in bulk PbSe cannot produce a significant enhancement of conversion efficiency. In contrast, for PbSe QDs with a quantized band gap of 0.95 eV, the maximum thermodynamic conversion efficiency is 31% for the SQ calculation, 37% for the L2 characteristic (solid green line), 32% for the L3 characteristic (solid purple line), and 42% for the M_{max} characteristic (solid red line). These calculations show that PbSe QDs will always have a much higher theoretical conversion efficiency compared to bulk PbSe (by factors ranging from 2.7 (L3 characteristic) to 3.5 (M_{max} characteristic)). The calculated conversion efficiencies also show that the maximum possible efficiency for present QDs (L3 characteristic) is barely enhanced compared to the SQ efficiency (32% vs 31%, respectively). However, if $h\nu_{th}$ can be reduced to $2E_g$ (L2 characteristic), the maximum efficiency is increased to 37%, and if the MEG QY characteristic can become staircase-like (M_{max}), the maximum conversion efficiency increases further to 42%. All these scenarios represent major increases of thermodynamic conversion efficiencies for PbSe QD solar cells compared to bulk PbSe solar cells. For MEG thresholds that are close to $2E_g$ the maximum conversion efficiency can be greatly enhanced over the SQ limit (ca. a 19% relative increase for L2 and ca. a 35% relative increase for M_{max}). We note that an M_{max} characteristic has been reported for MEG in the photocurrent measured in single single-walled carbon nanotubes (SWCNT), where after a photon energy threshold of $2E_g$ was reached, stepwise increases in photocurrent were measured at each subsequent increase of one E_g of applied voltage to the SWCNT p−n junction.[53] The research challenge for MEG in QD-based solar cells is to find materials and conditions that produce L2 and ultimately M_{max} MEG characteristics. Recent efforts toward producing efficient solar cells utilizing Pb−chalcogenide QDs as the active element show V_{oc} values that are higher than possible for a solar cell made from a bulk Pb−chalcogenide.[54,55] The higher band gap and resulting higher Voc attainable with QDs results in a higher PCE as seen in Figure 3. The higher EHPM efficiency in QDs vs bulk semiconductors allows for a lower $h\nu_{th}$ and thus drives the maximum possible PCE higher than the SQ limit for a bulk semiconductor of that given band gap.

Conclusions. We have shown that the correct way to compare EHPM processes between semiconductor QDs and bulk semiconductors is to plot the QY vs $h\nu/E_g$ as this provides a direct determination of the EHPM efficiency, η_{EHPM}, and allows for determination of the relative contributions of EHPM and competing relaxation channels. We show that there are large increases in theoretical thermodynamic photovoltaic conversion efficiencies for solar cells based on QDs compared to those based on bulk semiconductors. In contrast to previous publications,[8,25] we present data and detailed analyses in support of our belief that there are fundamental differences in the photophysics between EHPM processes in QDs and bulk semiconductors, in addition to major differences in theoretical solar conversion efficiency. The largest benefit to solar energy conversion would be a lowering of the photon energy onset for MEG, producing a staircase characteristic of QY vs $h\nu/E_g$. For nonideal cases, the energy onset relative to the band gap must be between 2 and $2.5E_g$ to have the greatest impact. We argue that the unique properties of QDs allow for lower threshold energy and higher η_{EHPM}. One theoretical study[56] surveyed 12 QD systems to determine which could produce an onset close to $2E_g$, and more such studies, both theoretical and experimental are needed along these lines.

Acknowledgment. We acknowledge helpful comments and discussion with Octavi Semonin and Justin Johnson. We

DOI: 10.1021/nl101490z | *Nano Lett.* **2010,** *10,* 3019–3027

thank Randy Ellingson for careful reading of the manuscript and discussion. M.C.B. and A.G.M. gratefully acknowledge funding from the Solar Photochemistry program within the Division of Chemical Sciences, Geosciences, and Biosciences in the Office of Basic Energy Sciences of the Department of Energy. M.C.H., J.M.L., B.K.H., and A.J.N. were supported as part of the Center for Advanced Solar Photophysics, an Energy Frontier Research Center funded by U.S. Department of Energy, Office of Science, Office of Basic Energy Sciences. DOE funding was provided to NREL through Contract DE-AC36-086038308.

REFERENCES AND NOTES

(1) Robbins, D. J. Aspects of the Theory of Impact Ionization in Semiconductors 0.1. *Phys. Status Solidi B* **1980**, *97* (1), 9–50.
(2) Landsberg, P. T. *Recombination in Semiconductors*; Cambridge University Press: Cambridge, 1991.
(3) Ellingson, R. J.; Beard, M. C.; Johnson, J. C.; Yu, P.; Micic, O. I.; Nozik, A. J.; Shabaev, A.; Efros, A. L. Highly Efficient Multiple Exciton Generation in Colloidal PbSe and PbS Quantum Dots. *Nano Lett.* **2005**, *5*, 865.
(4) Schaller, R.; Klimov, V. High Efficiency Carrier Multiplication in PbSe Nanocrystals: Implications for Solar Energy Conversion. *Phys. Rev. Lett.* **2004**, *92*, 186601.
(5) Califano, M.; Zunger, A.; Franceschetti, A. Direct carrier multiplication due to inverse Auger scattering in CdSe quantum dots. *Appl. Phys. Lett.* **2004**, *84* (13), 2409–2411.
(6) Trinh, M. T.; Houtepen, A. J.; Schins, J. M.; Hanrath, T.; Piris, J.; Knulst, W.; Goossens, A.; Siebbeles, L. D. A. In spite of recent doubts carrier multiplication does occur in PbSe nanocrystals. *Nano Lett.* **2008**, *8* (6), 1713–1718.
(7) Ji, M.; Park, S.; Conner, S. T.; Mokari, T.; Cui, Y.; Gaffney, K. J. Efficient Mulitple Exciton Generation Observed in Colloidal PbSe Quantum Dots with Temporally and Spectrally Resolved Intraband Excitation. *Nano Lett.* **2009**, *9* (3), 1217–1222.
(8) Nair, G.; Geyer, S. M.; Chang, L. Y.; Bawendi, M. G. Carrier multiplication yields in PbS and PbSe nanocrystals measured by transient photoluminescence. *Phys. Rev. B* **2008**, *78* (12), 10.
(9) Schaller, R. D.; Sykora, M.; Pietryga, J. M.; Klimov, V. I. Seven Excitons at a Cost of One: Redefining the Limits for Conversion Efficiency of Photons into Charge Carriers. *Nano Lett.* **2006**, *6*, 424.
(10) Murphy, J. E.; Beard, M. C.; Norman, A. G.; Ahrenkiel, S. P.; Johnson, J. C.; Yu, P.; Micic, O. I.; Ellingson, R. J.; Nozik, A. J. PbTe Colloidal Nanocrystals: Synthesis, Characterization, and Multiple Exciton Generation. *J. Am. Chem. Soc.* **2006**, *128*, 3241–3247.
(11) Beard, M. C.; Knutsen, K. P.; Yu, P. R.; Luther, J. M.; Song, Q.; Metzger, W. K.; Ellingson, R. J.; Nozik, A. J. Multiple exciton generation in colloidal silicon nanocrystals. *Nano Lett.* **2007**, *7* (8), 2506–2512.
(12) Schaller, R. D.; Petruska, M. A.; Klimov, V. I. Effect of electronic structure on carrier multiplication efficiency: Comparative study of PbSe and CdSe nanocrystals. *Appl. Phys. Lett.* **2005**, *87*, 253102.
(13) Schaller, R. D.; Sykora, M.; Jeong, S.; Klimov, V. I. High-Efficiency Carrier Multiplication and Ultrafast Charge Separation in Semiconductor Nanocrystals Studied via Time-Resolved Photoluminescence. *J. Phys. Chem B* **2006**, *110* (50), 25332–25338.
(14) Gachet, D.; Avidan, A.; Pinkas, I.; Oron, D. An Upper Bound to Carrier Multiplication Efficiency in Type II Colloidal Quantum Dots. *Nano Lett.* **2010**, *10* (1), 164–170.
(15) Schaller, R. D.; Pietryga, J. M.; Klimov, V. I. Carrier Multiplication in InAs Nanocrystal Quantum Dots with an Onset Defined by the Energy Conservation Limit. *Nano Lett.* **2007**, *7*, 3469–3476.
(16) Pijpers, J. J. H.; Hendry, E.; Milder, M. T. W.; Fanciulli, R.; Savolainen, J.; Herek, J. L.; Vanmaekelbergh, D.; Ruhman, S.; Mocatta, D.; Oron, D.; Aharoni, A.; Banin, U.; Bonn, M. Carrier Multiplication and Its Reduction by Photodoping in Colloidal InAs Quantum Dots. *J. Phys. Chem C* **2007**, *111* (11), 4146–4152.
(17) Stubbs, S. K.; Hardman, S. J. O.; Graham, D. M.; Spencer, B. F.; Flavell, W. R.; Glarvey, P.; Masala, O.; Pickett, N. L.; Binks, D. J. Efficient carrier multiplication in InP nanoparticles. *Phys. Rev. B* **2010**, *81* (8), 4.
(18) Gachet, D.; Avidan, A.; Pinkas, I.; Oron, D. An Upper Bound to Carrier Multiplication Efficiency in Type II Colloidal Quantum Dots. *Nano Lett.* **2010**, *10* (1), 164–170.
(19) Nair, G.; Bawendi, M. G. Carrier multiplication yields of CdSe and CdTe nanocrystals by transient photoluminescence spectroscopy. *Phys. Rev. B* **2007**, *76*, No. 081304.
(20) Pijpers, J. J. H.; Hendry, E.; Milder, M. T. W.; Fanciulli, R.; Savolainen, J.; Herek, J. L.; Vanmaekelbergh, D.; Ruhman, S.; Mocatta, D.; Oron, D.; Aharoni, A.; Banin, U.; Bonn, M. Carrier multiplication and its reduction by photodoping in colloidal InAs quantum dots. *J. Phys. Chem. C* **2007**, *111* (11), 4146–4152.
(21) Ben-Lulu, M.; Mocatta, D.; Bonn, M.; Banin, U.; Ruhman, S. On the absence of detectable carrier multiplication in a transient absorption study of InAs/CdSe/ZnSe core/shell1/shell2 quantum dots. *Nano Lett.* **2008**, *8* (4), 1207–1211.
(22) McGuire, J. A.; Joo, J.; Pietryga, J. M.; Schaller, R. D.; Klimov, V. I. New Aspects of Carrier Multiplication in Semiconductor Nanocrystals. *Acc. Chem. Res.* **2008**, *41* (12), 1810–1819.
(23) Beard, M. C.; Midgett, A. G.; Law, M.; Semonin, O. E.; Ellingson, R. J.; Nozik, A. J. Variations in the Quantum Efficiency of Multiple Exciton Generation for a Series of Chemically Treated PbSe Nanocrystal Films. *Nano Lett.* **2009**, *9* (2), 836–845.
(24) Midgett, A. G.; Hillhouse, H. W.; Hughes, B. K.; Nozik, A. J.; Beard, M. C. Submitted for publication.
(25) Pijpers, J. J. H.; Ulbricht, R.; Tielrooij, K. J.; Osherov, A.; Golan, Y.; Delerue, C.; Allan, G.; Bonn, M., Assessment of carrier-multiplication efficiency in bulk PbSe and PbS. *Nat. Phys.* **2009**, advance online publication.
(26) Shockley, W.; Queisser, H. J. *J. Appl. Phys.* **1961**, *32*, 510.
(27) Ross, R. T.; Nozik, A. J. Efficiency of Hot-Carrier Solar Energy Converters. *J. Appl. Phys.* **1982**, *53*, 3813.
(28) Hanna, M. C.; Nozik, A. J. Solar conversion efficiency of photovoltaic and photoelectrolysis cells with carrier multiplication absorbers. *J. Appl. Phys.* **2006**, *100*, 074510/1–074510/8.
(29) Alig, R. C.; Bloom, S.; Struck, C. W. Scattering by Ionization and Phonon Emission in Semiconductors. *Phys. Rev. B* **1980**, *22* (12), 5565–5582.
(30) Alig, R. C.; Bloom, S. Electron-Hole-Pair Creation Energies in Semiconductors. *Phys. Rev. Lett.* **1975**, *35*, 1522.
(31) http://en.wikipedia.org/wiki/Floor_and_ceiling_functions.
(32) Ridley, B. K., *Quantum Processes in Semiconductors*, 2nd ed.; Oxford University Press: New York, 1988.
(33) Tirino, L.; Weber, M.; Brennan, K. F.; Bellotti, E.; Goano, M. Temperature dependence of the impact ionization coefficients in GaAs, cubic SiC, and zinc-blende GaN. *J. Appl. Phys.* **2003**, *94* (1), 423–430.
(34) Ziaja, B.; London, R. A.; Hajdu, J. Ionization by impact electrons in solids: Electron mean free path fitted over a wide energy range. *J. Appl. Phys.* **2006**, *99* (3), 9.
(35) Jung, H. K.; Taniguchi, K.; Hamaguchi, C. *J. Appl. Phys.* **1996**, *79*, 2473.
(36) Delerue, C.; Allan, G.; Pijpers, J. J. H.; Bonn, M. Carrier Multiplication in bulk and nanocrystalline semiconductors: Mechanism, efficiency, and interest for solar cells. *Phys. Rev. B* **2010**, *81*, 125306.
(37) Klein, C. A. Bandgap dependence and Related Features of Radiation Ionization Energies in Semiconductors. *J. Appl. Phys.* **1968**, *39* (4), 2029.
(38) Kubarsepp, T.; Karha, P.; Ikonen, E. Interpolation of the spectral responsivity of silicon photodetectors in the near ultraviolet. *Appl. Opt.* **2000**, *39* (1), 9–15.
(39) Shabaev, A.; Efros, A. L.; Nozik, A. J. Multiexciton Generation by a Single Photon in Nanocrystals. *Nano Lett.* **2006**, *6*, 2856–2863.
(40) Nozik, A. J. Spectroscopy and Hot Electron Relaxation Dynamics in Semiconductor Quantum Wells and Quantum Dots. *Annu. Rev. Phys. Chem.* **2001**, *52*, 193.
(41) Nozik, A. J. Quantum dot solar cells. *Physica E* **2002**, *14* (1−2), 115–120.
(42) Efros, A. L.; Kharchenko, V. A.; Rosen, M. Breaking the phonon bottleneck in nanometer quantum dots: Role of Auger-like processes. *Solid State Commun.* **1995**, *93*, 281.

DOI: 10.1021/nl101490z | *Nano Lett.* **2010,** *10,* 3019–3027

(43) Blackburn, J. L.; Ellingson, R. J.; Micic, O. I.; Nozik, A. J. Electron relaxation in colloidal InP quantum dots with photo-generated excitons or chemically injected electrons. *J. Phys. Chem. B* **2003**, *107* (1), 102–109.
(44) Harbold, J. M.; Du, H.; Krauss, T. D.; Cho, K. S.; Murray, C. B.; Wise, F. W. Time-resolved intraband relaxation of strongly confined electrons and holes in colloidal PbSe nanocrystals. *Phys. Rev. B* **2005**, *72* (19), 195312.
(45) Guyot-Sionnest, P.; Wehrenberg, B.; Yu, D. Intraband relaxation in CdSe nanocrystals and the strong influence of the surface ligands. *J. Chem. Phys.* **2005**, *123*, 074709.
(46) Pandey, A.; Guyot-Sionnest, P. Slow Electron Cooling in Colloidal Quantum Dots. *Science* **2008**, *322*, 929.
(47) Klimov, V. I. Optical Nonlinearities and Ultrafast Carrier Dynamics in Semiconductor Nanocrystals. *J. Phys. Chem. B* **2000**, *104*, 6112–6123.
(48) Gali, A.; VoÏÏš, M. r.; Rocca, D.; Zimanyi, G. T.; Galli, G. High-Energy Excitations in Silicon Nanoparticles. *Nano Lett.* **2009**, *9* (11), 3780–3785.
(49) Schaller, R. D.; Agranovitch, V. M.; Klimov, V. I. *Nat. Phys.* **2005**, *1*, 189.
(50) Rupasov, V. I.; Klimov, V. I. Carrier multiplication in semiconductor nanocrystals via intraband optical transitions involving virtual biexciton states. *Phys. Rev. B* **2007**, *76* (12), 125321.
(51) Franceschetti, A.; An, J. M.; Zunger, A. Impact Ionization Can Explain Carrier Multiplication in PbSe Quantum Dots. *Nano Lett.* **2006**, *6* (10), 2191–2195.
(52) Klimov, V. I. Detailed-balance power conversion limits of nanocrystal-quantum-dot solar cells in the presence of carrier multiplication. *Appl. Phys. Lett.* **2006**, *89*, 123118.
(53) Gabor, N. M.; Zhong, Z. H.; Bosnick, K.; Park, J.; McEuen, P. L. Extremely Efficient Multiple Electron-Hole Pair Generation in Carbon Nanotube Photodiodes. *Science* **2009**, *325* (5946), 1367–1371.
(54) Ma, W.; Luther, J. M.; Zheng, H.; Wu, Y.; Alivisatos, A. P. Photovoltaic Devices Employing Ternary PbSxSe1-x Nanocrystals. *Nano Lett.* **2009**, *9* (4), 1699–1703.
(55) Luther, J. M.; Gao, J.; Lloyd, M. T.; Semonin, O. E.; Beard, M. C.; Nozik, A. J. Stability Assessment on a 3% Bilayer PbS/ZnO Quantum Dot Heterojunction Solar Cell. *Adv. Mat.* **2010**, DOI: 10.1002/adma.201001148.
(56) Luo, J. W.; Franceschetti, A.; Zunger, A. Carrier Multiplication in Semiconductor Nanocrystals: Theoretical Screening of Candidate Materials Based on Band-Structure Effects. *Nano Lett.* **2008**, *8* (10), 3174–3181.

DOI: 10.1021/nl101490z | *Nano Lett.* **2010,** *10,* 3019--3027